Journal of Saudi Chemical Society (2016) **20**, S591–S598

King Saud University

Journal of Saudi Chemical Society

www.ksu.edu.sa
www.sciencedirect.com

ORIGINAL ARTICLE

Synthesis, characterization and biological studies on some metal complexes with Schiff base ligand containing pyrazolone moiety

M. Sivasankaran Nair *, D. Arish, J. Johnson

Department of Chemistry, Manonmaniam Sundaranar University, Tirunelveli 627 012, India

Received 3 December 2012; accepted 18 April 2013
Available online 7 May 2013

KEYWORDS

Schiff base;
IR;
Electronic;
Antimicrobial;
DNA

Abstract 1:2 Complexes of Co(II), Ni(II), Cu(II) and Zn(II) with the Schiff base ligand Indal-4-AAP, derived from indole-3-carboxaldehyde and 4-aminoantipyrine were synthesized and characterized by elemental analyses, mass, IR, electronic spectra, magnetic moment, molar conductance and cyclic voltammetry. The complexes were found to have the general formulae $[ML_2Cl_2]$ (M = Co(II), Ni(II), Cu(II) and Zn(II)). The IR results demonstrate that the co-ordination sites are the azomethine nitrogen and carbonyl oxygen atoms of the Schiff base ligand. The electronic spectral and magnetic measurement data indicate that the complexes exhibit octahedral geometry around the metal center. The *in vitro* biological screening effects of the synthesized compounds were tested against various microbial species and the results show that the metal complexes are more biologically active than the ligand. The DNA cleavage activity of the ligand and its complexes was assayed on pUC18 DNA using gel electrophoresis. The result shows that Ni(II), Cu(II), and Zn(II) complexes have completely cleaved the DNA.

1. Introduction

The Schiff base ligands with nitrogen and oxygen donor atoms act as good chelating agents for the transition and non-transition metal ions (Singh et al., 2012; Wang et al., 2009; Mohanan et al., 2009). The interests in metal Schiff base complexes, particularly those of transition metal ions, are due to their potential applications in pharmaceutical and industrial fields (Paryzek et al., 2005; Kumar et al., 2009; Cozzi, 2004). The heterocyclic Schiff base ligands and their metal complexes have been the subject of extensive investigation because of their wide use in biological field (Dasilva et al., 2011; Chohan et al., 2010; Rosu et al., 2010; Raman et al., 2009). Transition metal complexes have been extensively studied for their nuclease-like activity using the redox properties of the metal and dioxygen to produce reactive oxygen species to promote DNA cleavage, yielding direct strand scission or base modification (Clever and Shionoya, 2010; Yang et al., 2010). Metal

* Corresponding author. Tel.: +91 9443540046; fax: +91 462 23334363.
E-mail addresses: msnairchem@rediffmail.com, hodchemmsu@yahoo.com (M. Sivasankaran Nair).
Peer review under responsibility of King Saud University.

ELSEVIER Production and hosting by Elsevier

http://dx.doi.org/10.1016/j.jscs.2013.04.007

complexes of nitrogen–oxygen chelating agents derived from 4-aminoantipyrine Schiff bases have pronounced applications in biological, clinical, analytical and pharmacological areas (Raja et al., 2012; El-Sonbati et al., 2012; Rosu et al., 2011; Mohamed et al., 2009). The present study deals with the synthesis, characterization and biological studies of the Schiff base (Indal-4-AAP) derived from indole-3-carboxaldehyde and 4-aminoantipyrine and its Co(II), Ni(II), Cu(II) and Zn(II) complexes.

2. Materials and methods

4-Aminoantipyrine and indole-3-carboxaldehyde were obtained from Sigma. Metal(II) chlorides were purchased from Merck. All other chemicals used were of AnalaR grade. Solvents were purified and distilled before use. The metal content in the complexes was determined by EDTA titration (Vogel, 1978). Elemental analysis was obtained using a Perkin-Elmer elemental analyzer. Conductivity measurements were made on freshly prepared 10^{-3} M solutions in DMSO at room temperature with a coronation digital conductivity meter. The IR spectra were recorded in KBr pellet on a JASCO FT/IR-410 spectrometer in the range 4000–400 cm^{-1}. Electronic spectra were recorded on a Perkin Elmer Lambda-25 UV/VIS spectrometer. The room temperature magnetic measurements were carried out using Guoy balance and the diamagnetic corrections were made using Pascal's constant (Kettle, 1969). Cyclic voltammetric measurements were carried out in a Bio-Analytical system (BAS) model CV-50W electrochemical analyzer. The three electrode cell comprised of a reference Ag/AgCl, auxiliary platinum and working glassy electrodes. Tetrabutylammonium perchlorate was used as supporting electrolyte.

2.1. Synthesis of Schiff base ligand (Indal-4-AAP)

An 1:1 equimolar methanolic solution of 4-aminoantipyrine (0.4064 g, 2 mmol) and indole-3-carboxaldehyde (0.2092 g, 2 mmol) was mixed and gently heated for 2 h after the addition of pinch of p-toluenesulphonicacid with constant stirring. The characteristic pale yellow precipitate obtained by Schiff base condensation was filtered out and kept for crystallization, dissolving in DMSO. Fine yellow crystals were obtained upon slow evaporation at room temperature. It was washed with alcohol, ether and dried in vacuum desiccator over anhydrous calcium chloride. The purity of the Schiff base was checked by TLC. (Yield: 87%).

2.2. Synthesis of metal Schiff base complexes

To the pale yellowish solution of Indal-4-AAP in 20 ml of THF (1.6555 g, 5 mmol) taken in a RB flask, a solution of metal(II) chloride in 20 ml of aqueous MeOH (5 mmol) was added dropwise with constant stirring. The reaction mixture was heated under reflux for 2 h and the volume was reduced to half of the initial volume under reduced pressure. The resultant precipitate was filtered, washed several times with cold EtOH, ether and then dried in vacuo over anhydrous $CaCl_2$ (Yield: 60–70%).

2.3. In vitro antimicrobial activity

Antibacterial and antifungal activities of the ligand and its complexes were tested *in vitro* against the bacterial species *Escherichia coli*, *Bacillus subtilis*, *Pseudomonas aeruginosa* and *Staphylococcus aureus*; fungal species, *Aspergillus niger*, *Aspergillus flavus*, and *Candida albicans* by the disk diffusion method (Bauer et al., 1966). Amikacin was used as the standard antibacterial agent, whereas Nystatin was used as the standard antifungal agent. The test organisms were grown on nutrient agar medium in petri plates. The compounds were prepared in DMF and soaked in filter paper disk of 5 mm diameter and 1 mm thickness. The disks were placed on the previously seeded plates and incubated at 37 °C and the diameter of inhibition zone around each disk was measured after 24 h for bacterial and 72 h for fungal species.

2.4. DNA cleavage analysis

The compounds were added separately to the pUC18 DNA sample. The sample mixtures were incubated at 37 °C for 2 h. The electrophoresis of the samples was done by weighing 300 mg of agarose and dissolving it in 25 ml of TAE buffer (4.84 g Tris base, pH 8.0, 0.5 M EDTA/1 L) by boiling. When the gel attained ~55 °C, it was poured into the gel cassette fitted with comb and allowed the gel to solidify. The comb was removed carefully and the gel was placed in the electrophoresis chamber flooded with TAE buffer. DNA sample (mixed with bromophenol blue dye at 1:1 ratio) was loaded carefully into

Table 1 Analytical and physical data of the Schiff ligand and its complexes.

Compound	Empirical formula	Color	Elemental analysis found (calcd)%				Λc (Ohm^{-1} cm^2 mol^{-1})	λ_{max} (nm)	μ_{eff} (B.M)
			C	H	N	M			
L	$C_{20}H_{18}N_4O$	Pale yellow	72.56 (72.71)	5.73 (5.49)	16.85 (16.96)	–	–	220, 270, 364	–
$[CoL_2Cl_2]$	$C_{40}H_{36}Cl_2N_8O_2Co$	Green	60.84 (60.77)	4.68 (4.59)	14.03 (14.17)	7.61 (7.45)	6.0	679, 613	5.13
$[NiL_2Cl_2]$	$C_{40}H_{36}Cl_2N_8O_2Ni$	Yellow	60.58 (60.79)	4.38 (4.59)	14.32 (14.18)	7.24 (7.43)	12.8	~1100, 779, 380	2.98
$[CuL_2Cl_2]$	$C_{40}H_{36}Cl_2N_8O_2Cu$	Brown	60.54 (60.41)	4.67 (4.56)	14.33 (14.09)	8.06 (7.99)	15.0	850, 380	1.92
$[ZnL_2Cl_2]$	$C_{40}H_{36}Cl_2N_8O_2Zn$	Yellow	60.65 (60.27)	4.41 (4.55)	13.95 (14.06)	8.37 (8.20)	14.0	220, 250, 326	Dia

the wells, along with standard DNA marker and constant 100 V of electricity was passed till the dye front reaches the end of gel. The gel was removed and carefully stained with ETBR solution (10 μg/ml) for 10–15 min and the bands under UV transilluminator were observed.

3. Results and discussion

3.1. Characterization of Schiff base ligand

The pale yellow colored Schiff base was found to be soluble in common organic solvents such as chloroform, THF, DMF and DMSO, but insoluble in methanol, ethanol and diethyl ether. The results of analytical data of the Schiff base ligand are given in Table 1 and the results are in good agreement with those calculated for the suggested formula. The observed sharp melting point of Indal-4-AAP is 284 °C which indicates the purity of the ligand. The DART mass spectrum of Indal-4-AAP (Fig. 1) shows a well-defined molecular ion peak at m/z = 331.14 (Relative Intensity = 18%), which coincides with formula weight of the Schiff base. The peak at m/z = 661.31 (2%) can be attributed to dimeric structure of the Indal-4-AAP. In addition, the spectrum of Indal-4-AAP shows a series of peaks at m/z = 204 (100%), 115 (16%), and 99 (20%) corresponding to its various fragments. The ^{1}H NMR spectrum of Indal-4-AAP is given in Fig. 2. The signal for azomethine proton (–CH═N–) in the ligand appears as a singlet at 9.747 ppm. The multiplet signals obtained in the 7.0–8.5 ppm range are due to the aromatic protons of Schiff base ligand. The signal for the pyrazolone ring carbon attached methyl proton ($-CH_3$) appears as a singlet at 2.5 ppm, while the pyrazolone ring nitrogen attached methyl protons ($>N-CH_3$) appears as a singlet at δ 3.3 ppm. The indole ring –NH proton appears as a singlet at 11.59 ppm. The IR spectrum of the ligand displays a sharp band at 1593 cm^{-1} which can be assigned to >C═N stretching frequency. Further, the Schiff base ligand exhibits a band at 1631 cm^{-1} due to υ(C═O). The electronic spectrum of the ligand shows a broad band at 364 nm, due to $\pi - \pi^*$ transition of the azomethine (>C═N) chromophore. In addition, the intense absorption band at higher energy, 270 nm, is presumably from the $\pi - \pi^*$ transition of the benzene ring of Indal-4-AAP.

3.2. Characterization of metal Schiff base complexes

The analytical data and physical properties of the metal Schiff base complexes are listed in Table 1. The complexes are stable toward air and moisture. All the complexes are soluble in MeOH, DMF, DMSO, and MeCN but insoluble in water. The analytical data indicate that the metal to ligand ratio is 1:2 for all the complex systems. The low conductivity values of the metal complexes (Table 1) suggest their non-electrolytic

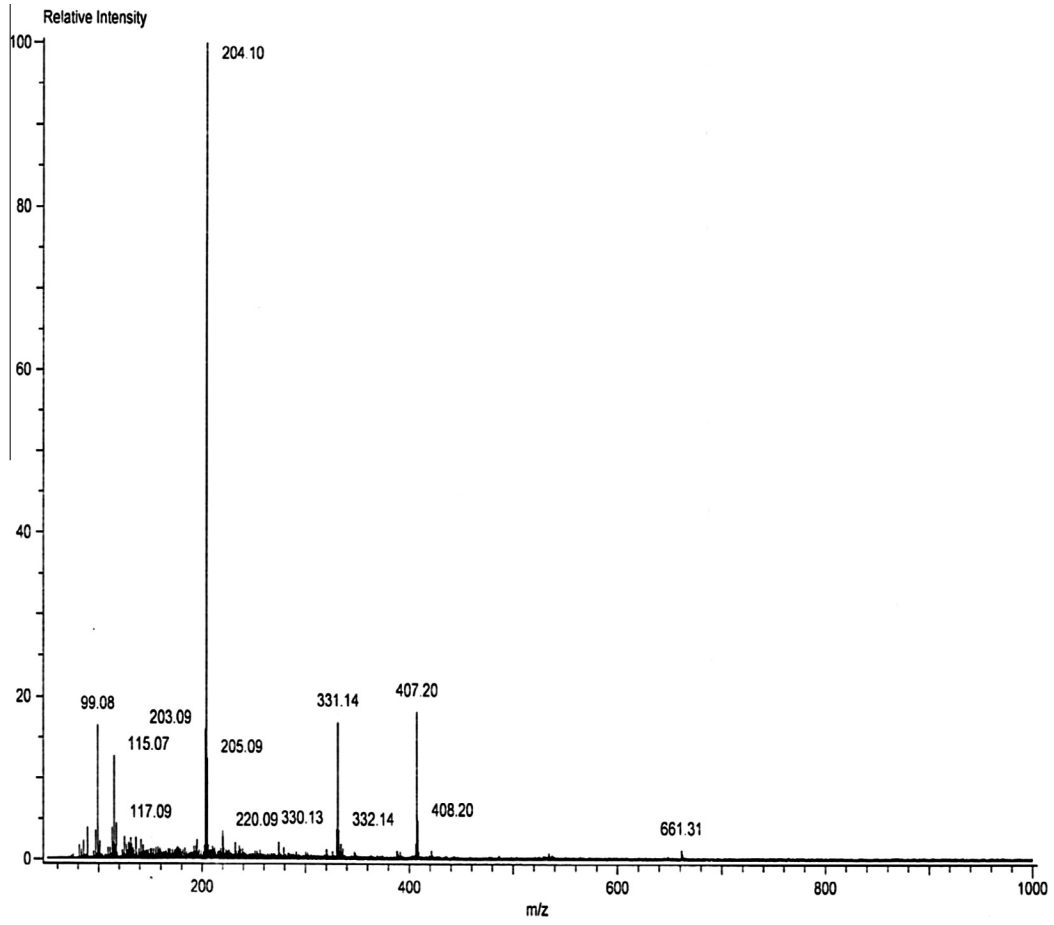

Figure 1 Mass spectra of Schiff base ligand.

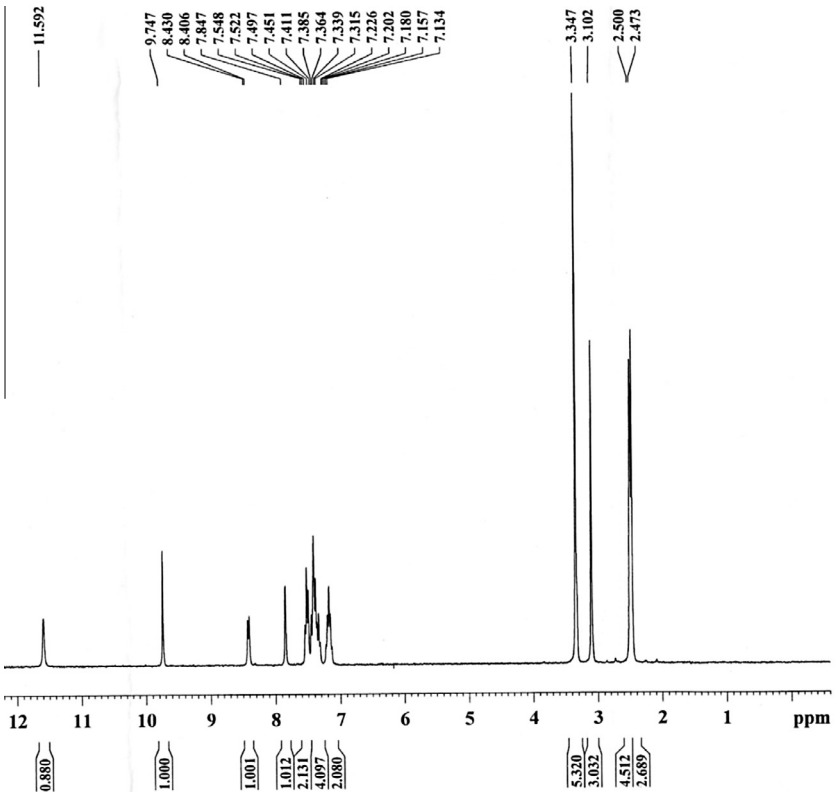

Figure 2 ^{1}H NMR spectra of Schiff base ligand.

Table 2 IR spectral data of the Schiff base ligand and its complexes (cm^{-1}).

Compound	υ_{azo}.(C═N)	υ(C═O)	υ_{ring}(C–N)	υ(M–O)	υ(M–N)
L	1593	1631	1242	–	–
$[CoL_2Cl_2]$	1573	1620	1210	515	451
$[NiL_2Cl_2]$	1584	1625	1242	508	456
$[CuL_2Cl_2]$	1580	1628	1242	508	456
$[ZnL_2Cl_2]$	1589	1626	1242	512	452

nature (Geary, 1971). The DART mass spectrum of Co(II), Ni(II), Cu(II), and Zn(II) complexes shows a peak at *m/z* 791.87 (10%), 791.07 (8%), 796.50 (11%) and 798.07 (14%) respectively, corresponding to their molecular weight. The mass spectrum of all the complexes indicates that the complexes are monomeric confirming the metal to ligand ratio to be 1:2 in the complexes.

3.3. ^{1}H NMR spectra

The ^{1}H NMR spectrum of Zn(II) complex was recorded at room temperature in DMSO D_6 solution. The azomethine proton in the complex shows a peak at 9.997, which is slightly downfield shift of 0.25 ppm. The shielding observed indicates the coordination of azomethine nitrogen atom to the Zn(II) ion. Compared to the Schiff base ligand, the Zn(II) complex shows a slight upfield shift of 0.01–0.15 ppm in the resonance peaks of the aromatic ring. Further, the indole ring –NH proton do not shift significantly in the spectrum of Zn(II) complex compared with the ligand which indicates that the indole nitrogen do not involve in the coordination.

3.4. IR spectra

The important IR spectral data are given in Table 2. On complexation the band at 1593 cm^{-1} for the azomethine group in the free ligand was shifted to a lower frequency in the range ~1589–1573, indicating the coordination of the azomethine nitrogen atom to the metal ion. The sharp band at 1631 cm^{-1} for υ(C═O) group of the free ligand has been shifted to ~1628–1620 cm^{-1} in the complex indicating the linkage between the metal ion and carbonyl oxygen atom. Further, the spectrum of all the complexes shows new bands in the 515–508 and 456–451 cm^{-1} regions, which may probably be due to the formation of M–O and M–N bonds, respectively (Ouf et al., 2010; Nakamoto, 1978).

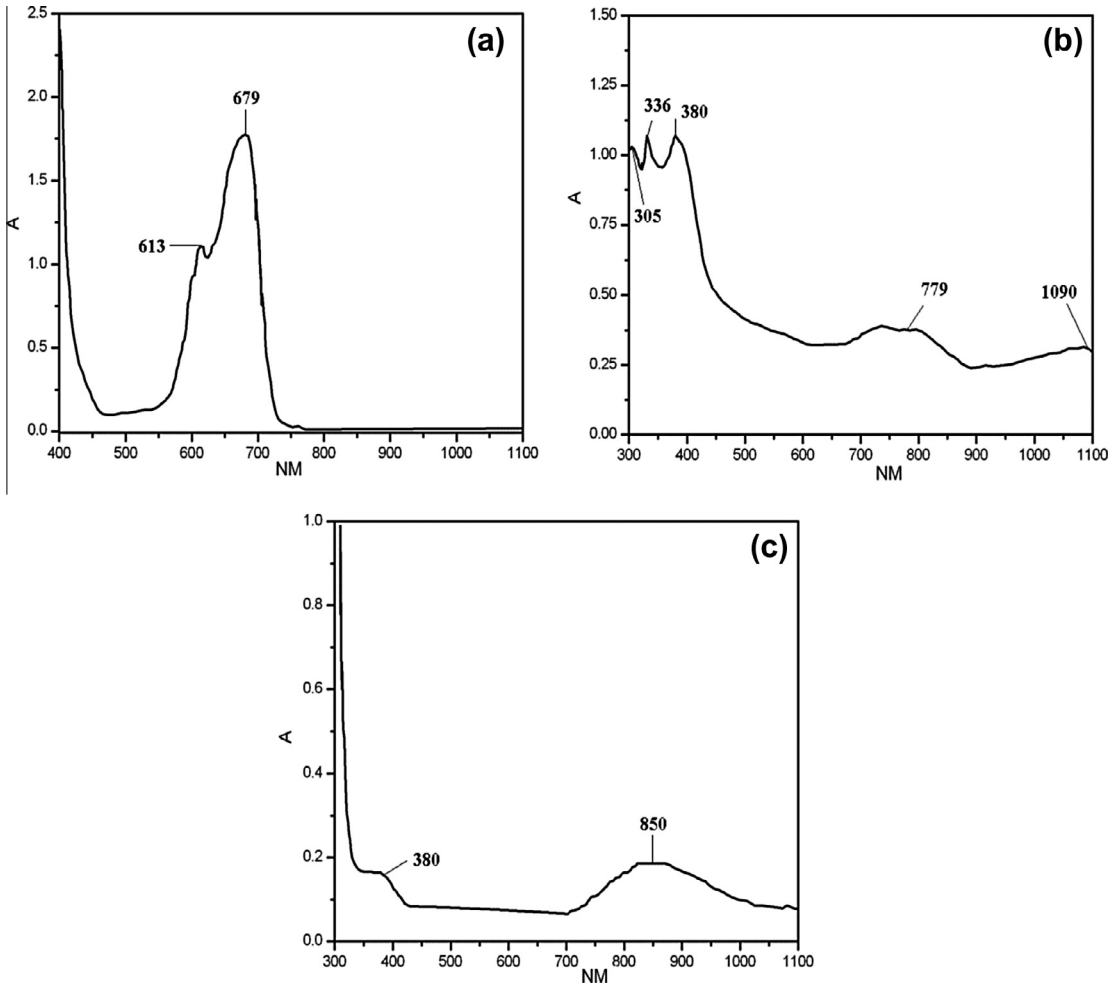

Figure 3 Electronic spectrum of (a) Co(II); (b) Ni(II), and (e) Cu(II) Schiff base complexes.

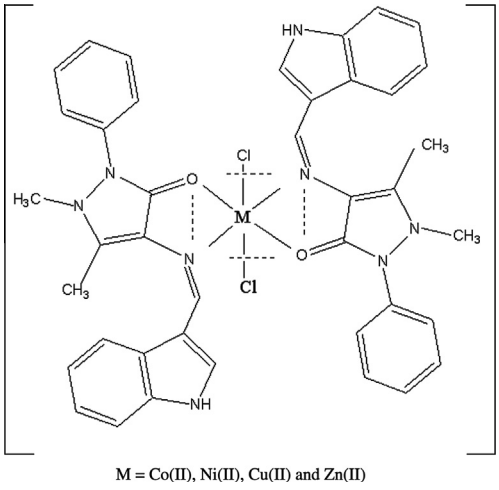

Figure 4 Proposed structure of Schiff base complexes.

3.5. Electronic spectra

The electronic spectrum of Co(II) complex (Fig. 3a) exhibits transitions at 679 and 613 nm respectively. The three possible d–d bands of high spin Co(II) octahedral complexes are $^4T_{1g}$ (F) $\rightarrow$ $^4T_{2g}$ (F), $^4T_{1g}$ (F) $\rightarrow$ $^4A_{2g}$ (F)) and $^4T_{1g}$ (F) $\rightarrow$ $^4T_{1g}$(P). The last transition will be highest in energy and may appear under the envelope of ligand-centered transitions (Nag et al., 2005). Thus the two transitions of the present Co(II) complex can be assigned to $^4T_{1g}$ (F) $\rightarrow$ $^4T_{2g}$ (F) and $^4T_{1g}$ (F) $\rightarrow$ $^4A_{2g}$ (F)) respectively, which demonstrates its octahedral geometry. The electronic spectrum of the Ni(II) complex shows (Fig. 3b) three bands in the region ~1100, 779, and 380 nm attributable to $^3A_{2g}$(F) $\rightarrow$ $^3T_{2g}$(F), $^3A_{2g}$(F) $\rightarrow$ $^3T_{1g}$(F) and $^3A_{2g}$(F) $\rightarrow$ $^3T_{1g}$(P) transitions respectively, suggesting an octahedral geometry around Ni(II) in the complex (Nag et al., 2005). The Cu(II) complex in their spectra displays a broad band centered at 850 nm and a weak shoulder at 380 nm region (Fig. 3c) due to ^2E_g $\rightarrow$ $^2A_{1g}$ and ^2E_g $\rightarrow$ $^2B_{1g}$ transitions, respectively, indicating the complex to have distorted octahedral geometry (Nag et al., 2005).

3.6. Magnetic measurements

The Co(II) complex has a magnetic moment of 5.13 BM (Table 1), which is in agreement with the reported value for octahedral Co(II) complexes (Banerjea, 1993; Kettle, 1969). The present Ni(II) complex shows a magnetic moment value of

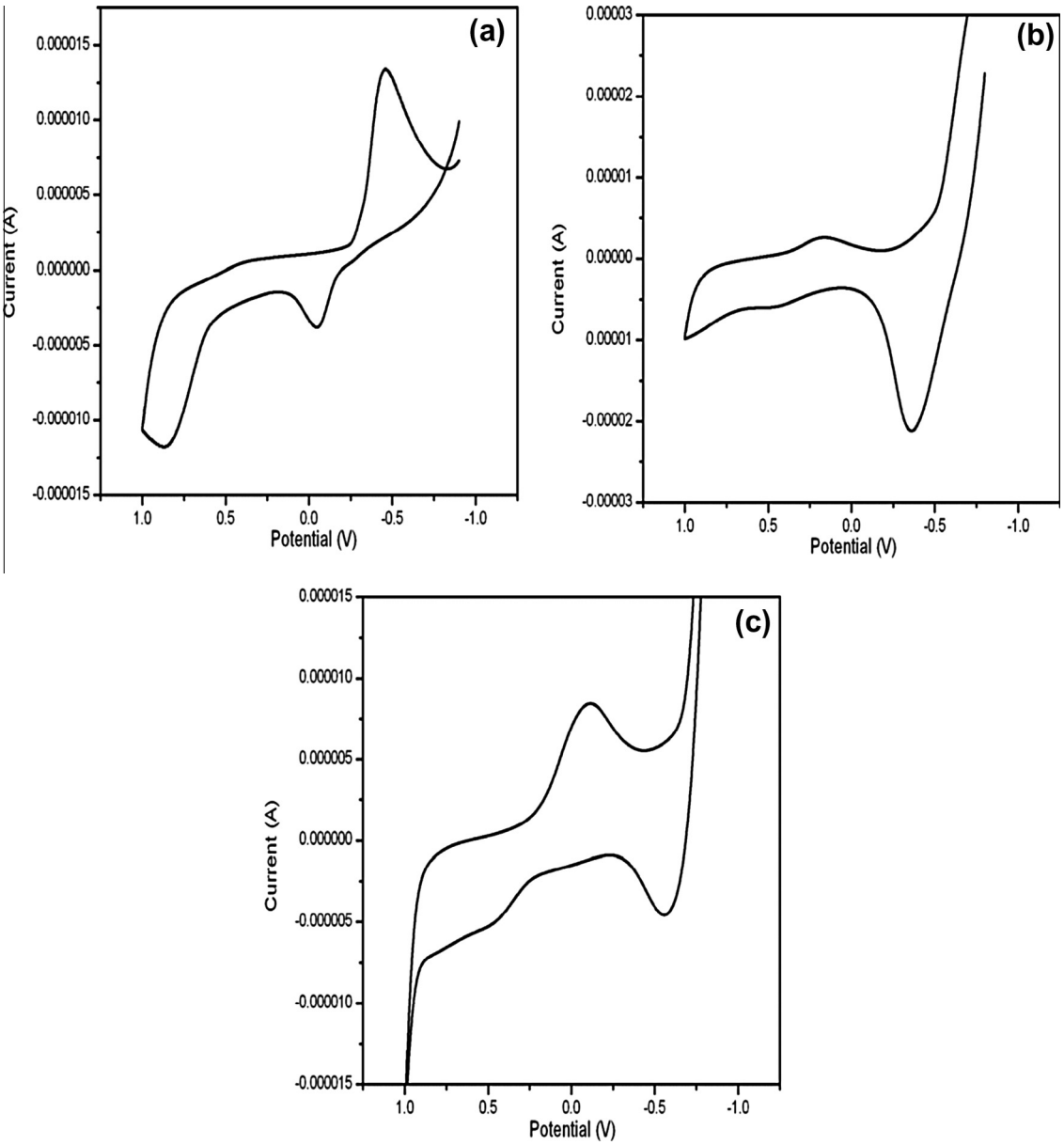

Figure 5 Cyclic voltammogram of (a) Co(II), (b) Ni(II), (c) Cu(II) Schiff base complexes.

2.98 within the range of 2.9–3.3 BM (Banerjea, 1993; Kettle, 1969) suggesting an octahedral environment. The Cu(II) complex shows a magnetic moment value of 1.92 BM, higher than the spin-only value 1.73 BM expected for one unpaired electron, monomeric and consistent with a distorted octahedral geometry (Banerjea, 1993; Kettle, 1969). The Zn(II) complex is diamagnetic and according to the empirical formulae of this complex, an octahedral geometry is proposed. Based on the above results, one can deduce the probable structures of the complexes as shown in Fig. 4.

3.7. Cyclic volumetric studies

All cyclic voltammograms were recorded in acetonitrile solution at a scan rate of 100 mVs^{-1} in the potential range from +2.0 to −2.0 V. The cyclic voltammogram of the Co(II) complex shows (Fig. 5a) a well defined redox process corresponding to the formation of the quasi-reversible Co(II)/Co(I) couple. The cathodic peak at −0.439 V versus Ag/AgCl and the associated anodic peak at −0.071 V correspond to the Co(II)/Co(I) couple. The peak to peak separation (ΔEp = 0.368 V) indicates a quasi-reversible one electron transfer process. The redox property of Ni(II) complex displayed (Fig. 5b) an irreversible anodic peak at −0.397 V, corresponding to the oxidation of Ni(II)/Ni(III). The irreversibility of the Ni(II)/Ni(I) was checked by varying the scan rates with peak potentials. The Cu(II) complex displayed (Fig. 5c) a cathodic peak at −0.103 V versus Ag/AgCl with the corresponding anodic wave at −0.609 V on the reverse scan. The peak separation value (ΔEp = 0.506 V) indicates a totally quasi-reversible character for the one electron transfer reaction of metal-based Cu(II)/Cu(I) couple. The free ligand and Zn(II)

Table 3 Antimicrobial activity results of the Schiff base ligand and its complexes.

Compound	Inhibition zone (μg/mL)						
	Bacteria species				Fungi species		
	S. aureus	*E. coli*	*P. aeruginosa*	*B. subtilis*	*C. albicans*	*A. niger*	*A. flavus*
L	–	12.5	10.2	–	–	–	–
$[CoL_2Cl_2]$	14.3	11.2	10.5	9.5	10.5	12.5	–
$[NiL_2Cl_2]$	12.5	12.5	12.2	–	11.5	11.5	10.5
$[CuL_2Cl_2]$	–	–	10.2	11.5	–	10.2	–
$[ZnL_2Cl_2]$	10.2	–	12.0	–	11.5	–	–
Amikacin[*]	19.2	20.5	20.5	18.5	–	–	–
Nystatin[*]	–	–	–	–	19.5	20.0	19.5

[*] Standard.

complex have not shown any peaks in this potential range under similar conditions.

4. Biological studies

4.1. *In vitro* antimicrobial activity

The *in vitro* biological screening results are given in Table 3. The standard error for the experiment is ±0.001 cm and the experiment is repeated three times under similar conditions. DMF is used as negative control and Amikacin is used as positive standard for antibacterial and Nystatin for antifungal activities.

From the results, it has been observed that the highest zones of inhibition i.e. 14.3, 11.2, and 10.5 mm were measured in *S. aureus*, *E. coli* and *P. aeruginosa* in case of Co(II) complex. Cu(II) complex shows highest inhibition zone (11.5 mm) against *B. subtilis*. Ni(II) complex shows intermediary inhibition zone against all the bacteria. The complexes show better antibacterial activity than their parental ligand and Co(II) complex has maximum and Cu(II) complex has least antibacterial effect. For antifungal activity (Table 3) the highest inhibitory zone (12.5 mm) was measured in Co(II) complex against *A. niger*. Again, Ni(II) complex shows intermediary inhibition zone against all the fungal species. The Zn(II) complex shows highest zone of inhibition 11.5 mm against *C. albicans*. The results show that the metal chelates are more toxic than their parent ligands against the same microorganism and under identical experimental conditions. The increase in antifungal activity of the metal chelates may be due to the effect of the metal ion on the normal cell process. A possible mode for toxicity increase may be considered in the light of Tweedy's chelation theory (Priya et al., 2009; Tweedy, 1964). On comparing the biological activity of the Schiff base and its metal complexes with the standard, it is seen that the biological activity follows the order; Ni(II) > Co(II) > Zn(II) > Cu(II) > L.

4.2. DNA cleavage studies

Gel electrophoresis experiments using pUC18 DNA were performed with ligand and its metal complexes in the presence and absence of H_2O_2 as an oxidant. The results given in Fig. 6 indicate that all the complexes can interact with pUC18 DNA in the presence of H_2O_2. Ni(II), Cu(II) and Zn(II) complexes are a potent chemical nuclease with higher nuclease activity than Co(II) as well as the free ligand. It was observed that most cleavage cases were due to the metal ions reacting with H_2O_2 to produce diffusible hydroxyl radicals or molecular oxygen, which might damage DNA through Fenton type chemistry (Babu et al., 2007). The general oxidative mechanisms proposed account for DNA cleavage by hydroxyl radicals via abstraction of a hydrogen from sugar units and predict the release of specific residues arising from transformed sugars, depending on the position from which the hydrogen atom is removed. The capacity of metal complexes to activate dioxygen, or its reduced form hydrogen peroxide, will lead to the functionalization of an inert C–H bond of DNA to a C–O bond. DNA oxidation by metal complexes occurs by C–H bond activation at the deoxyriboses (Pitie and Pratviel, 2010; Kellett, 2011). Further, control experiments show that the hydroxyl radical scavenger catalase or DMSO inhibits the DNA cleavage suggesting the possibility of hydroxyl radical as the reactive species.

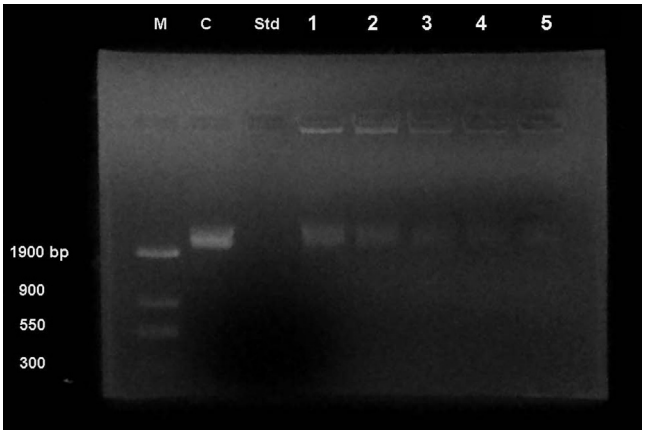

Figure 6 DNA cleavage studies of Schiff base ligand and its complexes, M- Marker, C- Control pUC 18 DNA (untreated sample), Std- 5 mM $FeSO_4$ treated DNA, 1- ligand + DNA + H_2O_2, 2- $[CoL_2Cl_2]$ + DNA + H_2O_2, 3- $[NiL_2Cl_2]$ + DNA + H_2O_2, 4- $[CuL_2Cl_2]$ + DNA + H_2O_2, 5-$[ZnL_2Cl_2]$ + DNA + H_2O_2.

5. Conclusion

Co(II), Ni(II), Cu(II), and Zn(II) complexes with the Schiff base ligand derived from indole-3-carboxaldehyde and 4-aminoantipyrine were synthesized and characterized by various physico-chemical methods. The analyses confirmed the composition and structures of the newly obtained complex combinations. The coordination of the Schiff base to the metal atom was found to be through the azomethine nitrogen, and the carbonyl oxygen atoms. The geometry of the complexes is assigned as octahedral. The Ni(II) and Co(II) complexes show better activity against most of the microbial species compared to that of ligand and other complexes. The DNA cleavage studies show that the Ni(II), Cu(II), and Zn(II) complexes have completely cleaved the DNA.

References

Babu, M.S.S., Reddy, K.H., Pitchika, G.K., 2007. Polyhedron 26, 572.
Banerjea, D., 1993. Coordination Chemistry. Tata McGraw-Hill.
Bauer, A.W., Kirby, W.M.M., Sherries, J.C., Truck, M., 1966. Am. J. Clin. Pathol. 45, 493.
Chohan, Z.H., Sumrra, S.H., Youssoufi, M.H., Hadda, T.B., 2010. Euro. J. Med. Chem. 45, 2739.
Clever, G.H., Shionoya, M., 2010. Coord. Chem. Rev. 254, 2391.
Cozzi, P.G., 2004. Chem. Soc. Rev. 33, 410.
daSilva, C.M., daSilva, D.L., Modolo, L.V., Alves, R.B., deResende, M.A., Martins, C.V.B., deFatima, A., 2011. J. Adv. Res. 2, 1.
El-Sonbati, A.Z., Diab, M.A., El-Bindary, A.A., El-Kader, M.K.A., 2012. Spectrochim. Acta. 99 (A), 211.
Geary, W.J., 1971. Coord. Chem. Rev. 7, 81.
Kellett, 2011. Dalton Trans. 40, 1024.
Kettle, S.F.A., 1969. Coordination Compounds. ELBS, Essex, UK.
Kumar, S., Dhar, N.D., Saxena, N.P., 2009. J. Sci. Ind. Res. 68, 181.
Mohamed, G.G., Omar, M.M., Ibrahim, A.A., 2009. Euro. J. Med. Chem. 44, 4801.
Mohanan, K., Athira, C.J., Sindhu, Y., Sujamol, M.S., 2009. J. Rare Earths 29, 705.
Nag, J.K., Pal, S., Sinha, C., 2005. Trans. Met. Chem. 30, 523.
Nakamoto, K., 1978. Infra-Red and Raman Spectra of Inorganic and Coordination Compounds, third ed. John Wiley, New York.
Ouf, A.E.L., Ali, M.S., Saad, E.M., Mostafa, S.I., 2010. J. Mol. Struct. 973, 69.
Paryzek, W.R., Patroniak, V., Lisowski, J., 2005. Coord. Chem. Rev. 249, 2156.
Pitie, M., Pratviel, G., 2010. Chem. Rev. 110, 1018.
Priya, N.P., Arunachalam, S.V., Sathya, N., Chinnusamy, V., Jayabalakrishnan, C., 2009. Trans. Met. Chem. 34, 437.
Raja, G., Butcher, R.J., Jayabalakrishnan, C., 2012. Spectrochim. Acta. 94 (A), 210.
Raman, N., Raja, S.J., Sakthivel, A., 2009. J. Coord. Chem. 62, 691.
Rosu, T., Negoiu, M., Pasculescu, S., Pahontu, E., Poirier, D., Gulea, A., 2010. Euro. J. Med. Chem. 45, 774.
Rosu, T., Pahontu, E., Maxim, C., Georgescu, R., Stanica, N., Gulea, A., 2011. Polyhedron 30, 154.
Singh, B.K., Rajour, H.K., Prakash, A., 2012. Spectrochim. Acta. 94 (A), 143.
Tweedy, B.G., 1964. Phytopathology 25, 910.
Vogel, A.I., 1978. A Textbook of Quantitative Inorganic Analysis Including Elementary Instrumental Analysis, fourth ed. Longman, London.
Wang, Q., Yang, Z.Y., Qi, G.F., Qin, D.D., 2009. Euro. J. Med. Chem. 44, 2425.
Yang, H., Metera, K.L., Sleiman, H.F., 2010. Coord. Chem. Rev. 254, 2403.